Study on the ideal location of a bottom drainage roadway

by H. Chen[1,2,3], F. An[1,2,3], Z. Wang[1], and X. Chen[1]

Affiliation:
[1]State Key Laboratory Cultivation Base for Gas Geology and Gas Control, Henan Polytechnic University, China.
[2]Henan Key Laboratory of Coal Green Conversion, Henan Polytechnic University, China.
[3]Collaborative Innovation Center of Coal Safety Production of Henan Province, China.

Correspondence to:
F. An

Email:
anfenghua999@126.com

Dates:
Received: 8 Mar. 2021
Revised: 11 Jan. 2022
Accepted: 4 Apr. 2022
Published: May 2022

How to cite:
Chen, H., An, F., Wang, Z., and Chen, X. 2022
Study on the ideal location of a bottom drainage roadway.
Journal of the Southern African Institute of Mining and Metallurgy, vol. 122, no. 5, pp. 259-266

DOI ID:
http://dx.doi.org/10.17159/2411-9717/1561/2022

ORCID:
H. Chen
https://orcid.org/0000-0001-7630-0200
F. An
https://orcid.org/0000-0002-5902-6761
Z. Wang
https://orcid.org/0000-0002-4615-4617
X. Chen
https://orcid.org/0000-0003-0753-5609

Synopsis

The bottom drainage roadway plays a crucial role in preventing coal and gas outbursts by using underground gas drainage methods. Therefore, it is essential to select the ideal position of the bottom drainage roadway. In this paper use a combination of geological data and numerical simulation to study the ideal position of the bottom drainage roadway, we taking the gas drainage of the first workface of No. 3 coal seam in the Yuxi coal mine in China as an example. The geological study showed a limestone marker layer at an average vertical distance of 14 m from the first mining face. Using this marker layer, the bottom drainage roadway could be excavated without the risk of accidentally exposing the coal seam, and less crosscutting borehole drilling from the bottom drainage roadway would be required. Based on the needs of gas control, the layout of the bottom drainage roadway was selected as an external stagger type. Combined with the numerical simulation results, when located 20 m outside of the mining workface 'footprint' on the horizontal projection, the bottom drainage roadway was a sufficient distance from the stress concentration area during mining of workface 1301, which facilitated roadway maintenance. Furthermore, the length of the crosscutting boreholes is also relatively short, which reduces the amount and cost of drilling. The results of this study are expected to provide a reference for the selection of an ideal position of the bottom drainage roadway in field engineering.

Keywords

gas drainage; bottom drainage roadway; geological analysis; numerical simulation.

Introduction

China has one of the highest rates of serious coal and gas outbursts in the world (Chen *et al*., 2014, 2017; Lu *et al*., 2017, 2019). Years of coal mining have proven that pre-draining of coal gas effectively prevents coal and gas accidents (Cheng *et al*., 2010; Guo *et al*., 2012; Kong *et al*., 2014; Jiang *et al*., 2019; Wang *et al*., 2020). Drilling of boreholes for gas drainage also reduces the *in-situ stress in the coal seam.* After the gas is extracted, the gas energy storage in the coal body is reduced. Importantly, after the gas pressure decreases, the coal strength would be increased (Cheng *et al*., 2010). Therefore, by applying technology for pre-draining of coal gas, the main factors related to both coal and gas outbursts are weakened (Xue *et al*., 2014; Yu *et al*., 2015; Li *et al*., 2017; Yang *et al*., 2018). Among pre-draining methods, a combination of crosscutting boreholes and bedding boreholes extraction is commonly used, as shown in Figure 1 (Wang *et al*., 2014; Chen *et al*., 2017).

With a combination of crosscutting borehole extraction and bedding borehole extraction, the choice of bottom drainage roadway location is crucial, directly affecting the reliability of outburst elimination measures and the amount of drilling required (Chen *et al*., 2018; Pan *et al*., 2019; Yang *et al*., 2019). When selecting the position of the bottom drainage roadway, the stability of the roadway must be considered. Yang *et al*. (2017), Bai *et al*. (2016), Zhang *et al*. (2013), Whittaker and Singh (1981), Zhang *et al*. (2015), Jiang *et al*. (2016), Islam and Shinjo (2009), Dejean (1976), and Xiao *et al*. (2014) analysed the effect of floor stress evolution, pillar size, and tectonic stress on roadway stability. Coggan *et al*. (2012) found that the thickness of the relatively weak mudstone in the roadway roof had a significant influence on the extent of failure. Wang *et al*. (2015) assessed the excavation damaged zone around roadways under dynamic pressure induced by an active mining process. Through numerical and physical simulations, Xie and Xu (2015) studied the feasibility of using ground penetrating radar-based detection to monitor roadway roof separation.

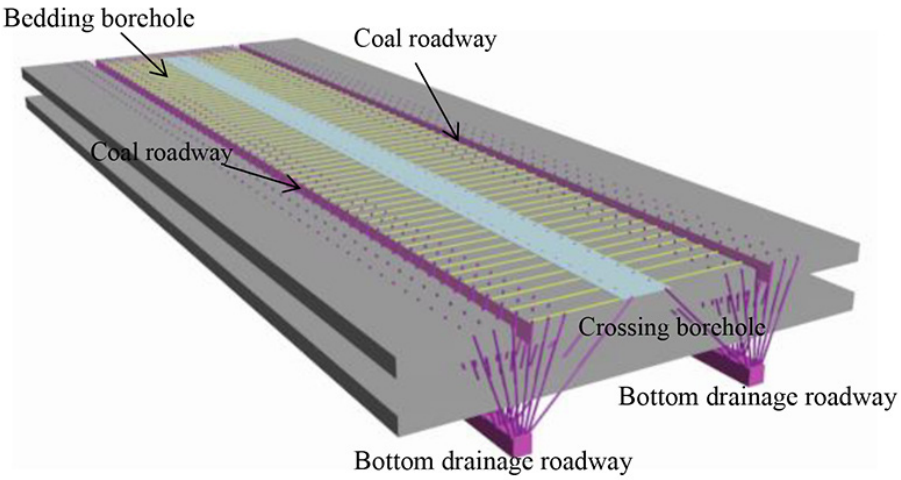

Figure 1—Combination of outburst prevention measures of crosscutting boreholes extraction and bedding boreholes for gas pre-drainage in the workface (modified from Wang *et al.*, 2014)

As regards the specific selection method for locating of the bottom drainage roadway, Liu, Li, and Pan (2016) analysed the floor stress distribution characteristics of the working face, and studied the layout of the bottom drainage roadway under the condition of closely-spaced coal seam groups. Nan, Li, and Guan (2015) determined the optimal location of the bottom drainage roadway based on the characteristics of roadway deformation obtained by numerical simulation combined with economic factors. Liu and Zhang (2018) established a floor failure depth model, and calculated the vertical distance between the bottom drainage roadway and the coal seam floor through numerical simulation. They also determined the horizontal distance between the bottom drainage roadway and the working face. Li and Li (2015) conducted on-site measurements of the deformation of the roadway during the mining of the workface to provide a basis for the selection of the ideal location of the bottom drainage roadway.

Due to the differences in geological characteristics, gas occurrence, and gas control modes in different coal mines, the methods used to determine the location of the bottom drainage roadway would be also be different. In this paper, a combination of geological surveys and numerical simulations is used to determine the location of the bottom drainage roadway for the first mining workface of No. 3 coal seam in the Yuxi coal mine in China,. The results of this study are expected to provide a reference for the selection of the ideal position of the bottom drainage roadway under similar conditions.

Research background

This study is based on the mining practice at the Yuxi coal mine in Shanxi Province, China. The main recoverable coal seams are the No. 3 and No. 15 seams with a layer spacing of 87.5 m. The No. 3 coal seam, with a permeability of 13.3416 $m^2 \cdot (MPa2 \cdot d)^-$, was mined first and embodies the risk of coal and gas outbursts. The maximum original gas content and pressure of the No. 3 seam were 25.59 m^3/t and 2.90 MPa, respectively.

The first mining workface of the No. 3 coal seam is workface 1301, and U-type ventilation is used. Considering the outburst risk of the No. 3 coal seam, a combination of outburst prevention measures compriing crosscutting borehole extraction and bedding borehole extraction was used. The procedure followed is shown in Figure 2. The bottom drainage roadway was excavated first, and

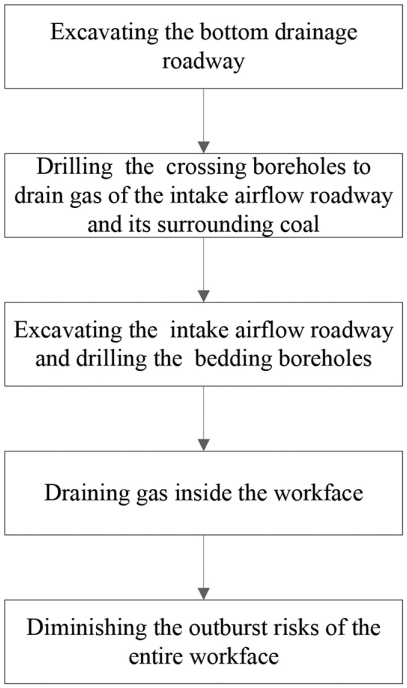

Figure 2—Schematic diagram showing the procedure for implementing the outburst prevention measures

the crosscutting boreholes with spacing of 5-10 m were drilled to 15 m outside the intake airflow roadway contour line though the bottom drainage roadway to drain gas from the intake airflow roadway and surrounding coal. When the residual gas content is reduced to less than 8 m^3/t (China State Administration of Work Safety, 2019), the intake airflow roadway can be excavated. Then, by using a ZDY6000 LD hydraulic directional drilling rig, bedding boreholes for draining gas inside the workface could be drilled in the intake airflow roadway, and boreholes with a spacing of 10~15 m were bored to 15 m outside the return airflow roadway and open-off cut. Each drilling operation was designed with one or two branches. The layout of the gas drainage boreholes is shown in Figure 3.

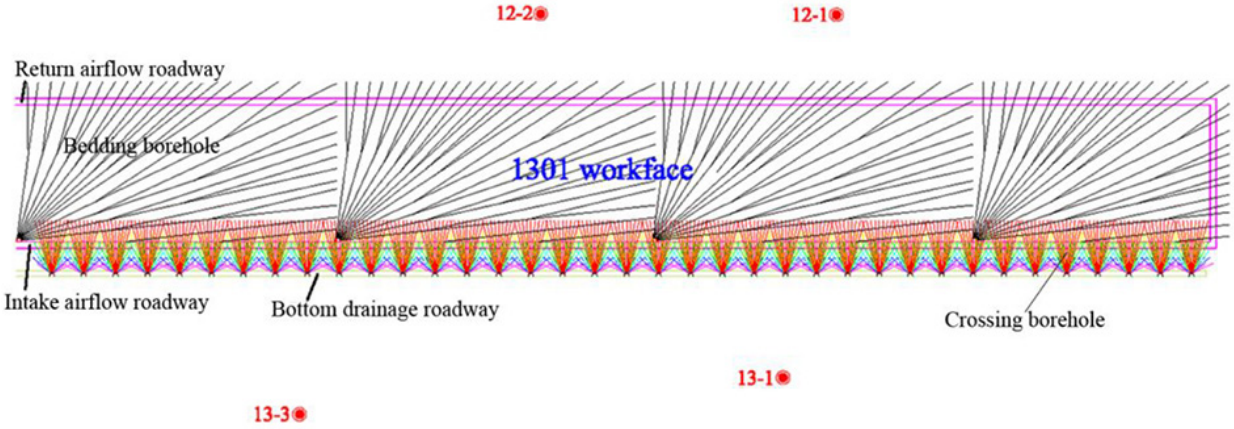

Figure 3—Arrangement of outburst prevention measures in workface 1301

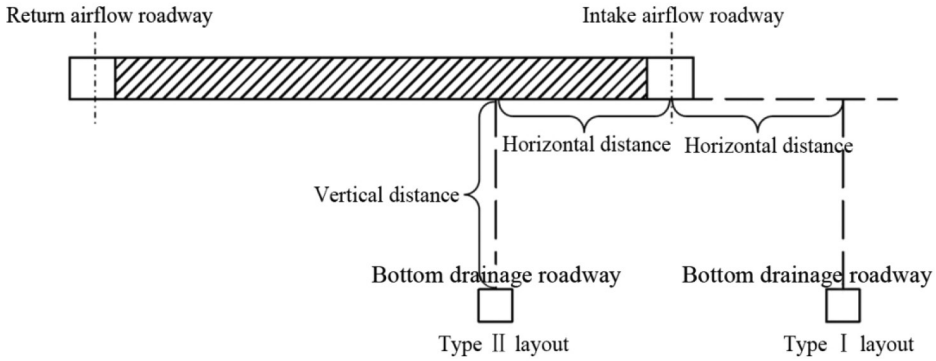

Figure 4—Layout styles for bottom drainage roadway

Figures 2 and 3 show the importance of positioning the bottom drainage roadway appropriately. If it is too close to the coal seam, the seam can be easily exposed unintentionally during roadway excavation. If it is too far away from the seam in the vertical direction, the crosscutting boreholes will be too long, which will not only lead to wasteful borehole drilling but also cause safety problems such as creating 'drainage blind areas' caused by borehole deviations and inaccurate positioning. Owing to the above problems, it is necessary to determine the ideal position of the bottom drainage roadway for gas drainage.

Determination of the ideal position of the bottom drainage roadway

There are two layout styles for bottom drainage roadways, as shown in Figure 4: type I and type II. Type I layout requires the bottom drainage roadway to be outside of the mining workface 'footprint' on the horizontal projection. Conversely, type II locates the bottom drainage roadway inside the mining workface 'footprint' on the horizontal projection. Determining an ideal location for the bottom drainage roadway involves selecting the appropriate bottom drainage roadway layout style and the vertical and horizontal distances between the bottom drainage roadway and the mining workface.

As workface 1301 is the first mining workface of the No. 3 coal seam, the type I layout style was selected for the bottom drainage roadway, which meets the needs of constructing crosscutting boreholes for workface 1301 and the adjacent workface.

Basic principles of selecting the position of bottom drainage roadways

When the position of the bottom drainage roadway is selected, the following principles should be followed:

(1) Identify a marker bed to easily locate the roadway.
(2) Coal seams must not be accidentally exposed during excavation of the bottom drainage roadway.
(3) To facilitate maintenance, the bottom drainage roadway should be arranged located in a competent rock formation.
(4) Appropriate positioning of the bottom drainage roadway can reduce the number of crosscutting boreholes, saving coal mining costs.

Determination of the vertical distance between the bottom drainage roadway and the mining workface

In this section, the results of a geological survey were used to determine the vertical distance between the bottom drainage roadway and the mining workface. Four geological exploration drill-holes were completed around the 1301 workface (Figure 3), namely 12-1, 12-2, 13-1, and 13-3. Data from 13-1 is missing, and schematic logs of the other geological exploration drill-holes are shown in Figures 5-7. Figure 5 and Figure 6 show that limestone is present at 12.59 m and 14.67 m below the No. 3 coal seam. Since the 12-2 geological exploration borehole (Figure 7) was drilled to 11.95 m below the No. 3 coal seam, the limestone was not intersected.

Rock thickness (m)	Depth (m)	Columnar	Lithology
0.93	681.25		Siltstone
5.63	687.05		3# coal seam
4.05	691.10		Siltstone
2.50	693.60		Mudstone
1.30	694.90		Fine sandstone
4.74	699.64		Sandy mudstone
1.20	700.84		Limestone

Figure 5—Schematic log of geological exploration borehole 12-1

Rock thickness (m)	Depth (m)	Columnar	Lithology
0.73	508.28		Mudstone
0.70	508.98		Carbonaceous mudstone
5.63	514.61		3# coal seam
1.00	515.61		Siltstone
2.87	518.48		Fine sandstone
5.40	523.88		Siltstone
1.80	525.68		Fine sandstone
3.60	529.28		Sandy mudstone
1.30	530.58		Limestone

Figure 6—Schematic log of geological exploration borehole 13-3

Rock thickness (m)	Depth (m)	Columnar	Lithology
0.60	711.94		Sandy mudstone
6.30	718.24		3# coal seam
0.50	718.74		Sandy mudstone
3.50	722.24		Siltstone
7.55	729.79		Mudstone
0.20	729.99		Coal seam
0.20	730.19		Mudstone

Figure 7—Schematic log of geological exploration borehole 12-2

Therefore, the bottom drainage roadway is located approximately 14 m below the No. 3 coal seam with a limestone roof. This has the following benefits.

(1) The layer thickness between the bottom drainage roadway and the No. 3 coal seam is up to 14 m. This meets the requirements of Detailed Rules for Prevention and Control of Coal and Gas Outburst (China State Administration of Work Safety, 2019), namely, that all the rock roadways excavations close to a coal seam with an outburst risk must be explored to ensure a minimum distance of no less than 5 m between the roadway and the coal seams.

(2) The limestone can be used as the marker bed during excavation of the bottom drainage roadway so that the coal seam cannot be exposed inadvertently, resulting in a coal and gas outburst accident.

(3) The bottom drainage roadway is located in sandy mudstone, which is beneficial for the maintenance of the roadway.

Determination of the horizontal distance between the bottom drainage roadway and mining workface

The bottom drainage roadway serves as a site from which to drill not only the crosscutting boreholes for workface 1301, but also those for the adjacent workface. Therefore, in order to ensure that the crosscutting boreholes through workface 1301 and the adjacent workface are as short as is practical, the bottom drainage roadway should be located in the middle of the coal pillar between the two workfaces as far as practical on the horizontal projection. In addition, the roadway should be located away from the stress concentration area to facilitate stability.

To clarify the stress distributions of the surrounding rock, FLAC3D numerical simulation software was used. This software uses an explicit finite difference scheme to analyse deformation problems (Itasca Consulting Group, 2005).

Numerical calculation model and boundary conditions

The mechanical parameters used in the simulation are shown in Table I. The depth of the coal seam is 600 m, and a compressive stress of 12 MPa was imposed at the top of the model. The other sides of the model were given rolling boundaries with an imposed stress of 10 MPa. A fixed boundary was defined at the bottom of the model.

The Mohr-Coulomb model was selected for use, and the numerical calculation model is shown in Figure 8. The length, width, and height of the model are 405 m, 350 m, and 77.02 m, respectively. The mining length simulated is 150 m, extending from 100 m to 250 m in the x-direction. The mining width is 205 m, extending from 100 m to 305 m in the y-direction, and the mining height is 5.85 m. The model contains 78 000 zones and 83 997 grids.

Table 1

Integrated histogram and mechanical parameters of the experimental coal mine

Lithology	Elastic modulus [GPa]	Shear modulus [GPa]	Friction Angle [°]	Cohesion [MPa]	Tensile strength [MPa]	Thickness [m]
Medium-granite sandstone	12.30	12.50	30.50	25.70	8.00	14.58
Mudstone	8.30	4.80	22.01	6.53	4.89	5.65
Medium-granite sandstone	12.30	12.50	30.50	25.70	8.00	3.93
Siltstone	11.90	11.40	26.90	16.68	6.86	4.66
No. 3 coal seam	3.30	0.71	30.00	8.00	2.00	5.85
Siltstone	11.90	11.40	26.90	16.68	6.86	1.38
Mudstone	8.30	4.80	22.01	6.53	4.89	7.82
Sandy mudstone	9.63	5.71	28.65	9.12	5.23	4.13
Limestone	15.90	11.40	20.90	20.68	10.20	1.21
Sandy mudstone	9.63	5.71	28.65	9.12	5.23	27.81

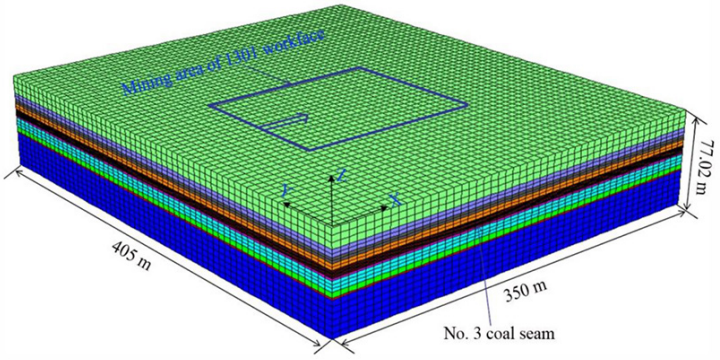

Figure 8—Numerical calculation model

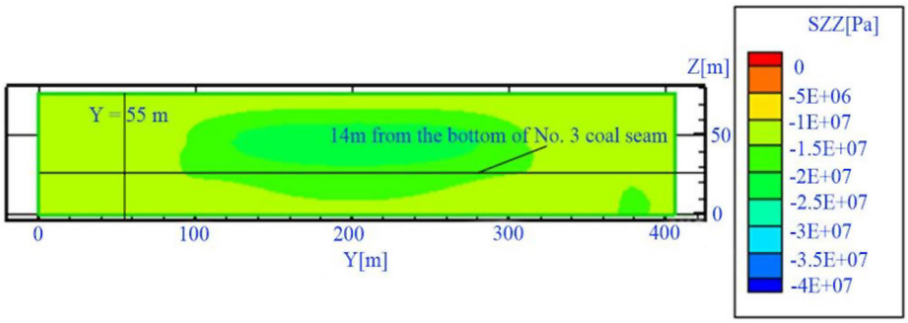

Figure 9—Stress distribution in the z-direction with the 1301 workface mined 15 m away from the reference plane

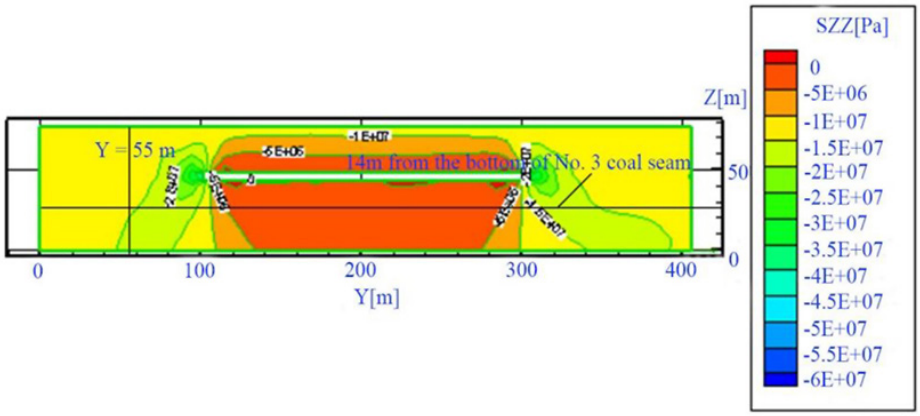

Figure 10—Stress distribution in the z-direction with the 1301 workface mined 25 m behind the reference plane

Stress evolution of the surrounding rock during mining of the 1301 workface

For the purposes of the exercise, the plane at x = 175 m is chosen as the reference plane. Since the stress distributions of the surrounding rock in the x-, y-, and z-directions are similar (Chen *et al.*, 2014), only the stress distributions of the reference plane in the z-direction are shown (Figures 9-11).

According to Figures 9-11, the following characteristics will be obtained while mining the 1301 workface.

(1) The stress state of the surrounding rock is a stress concentration area, stress increase area, and original stress area from the intake airflow roadway of workface 1301 outward.

(2) When the workface is mined to 45 m behind the reference plane, the 14 m vertical distance from the coal seam floor and the y = 55 m contour exactly intersects the edge of the original stress area. According to the model, the actual location is 55 m away from the intake airflow roadway of workface 1301. The range of the stress concentration area is approximately 0–10 m.

The coal pillar between workface 1301 and the adjacent workface is 40 m wide. In line with the previous analysis, the bottom drainage roadway for gas drainage should be located 20 m away from the intake airflow roadway of workface 1301 on the horizontal projection. According to the numerical simulation results, when located 20 m outside the mining workface 'footprint'

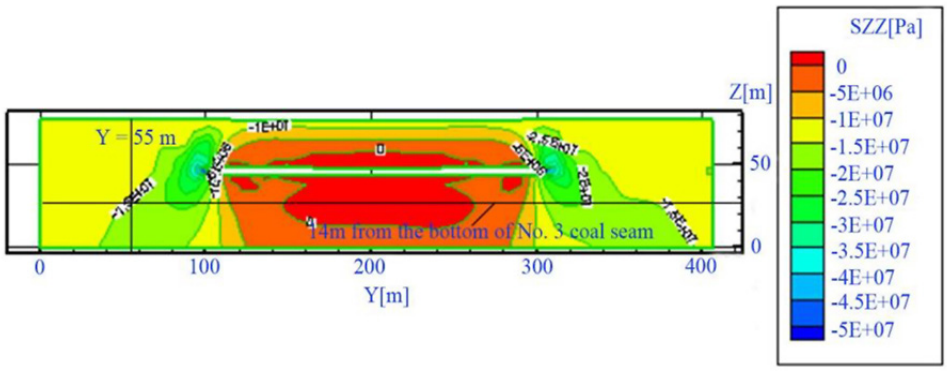

Figure 11—Stress distribution in the z-direction with the 1301 workface mined 45 m behind the reference plane

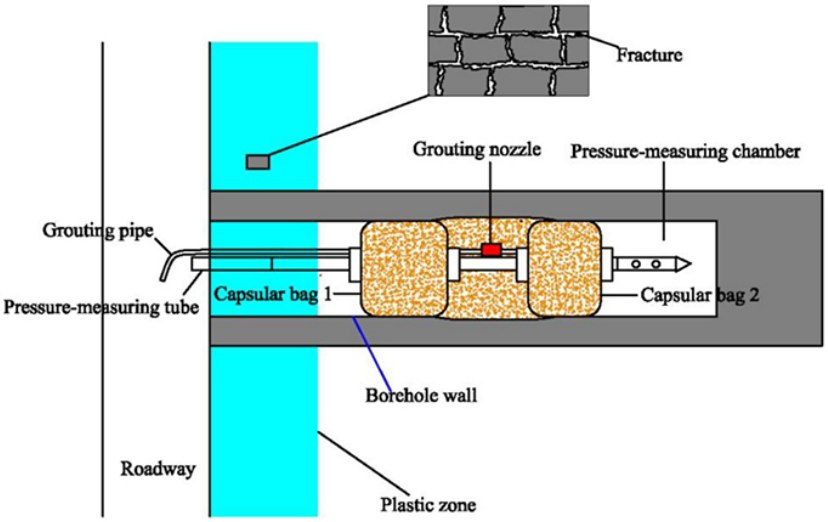

Figure 12—Schematic diagram of borehole sealing and plastic zone (Sun *et al.*, 2015; Hu and Liu 2016; Chen *et al.*, 2020)

on the horizontal projection, the bottom drainage roadway will be outside the stress concentration area during mining of workface 1301, which facilitates roadway maintenance. Furthermore, the length of the crosscutting boreholes is relatively short, which reduces the amount and cost of drilling. This is also consistent with the statistical results for bottom drainage roadway location in outburst-prone mines in China (Cheng, 2010).

Discussion

Plastic zone range of the bottom drainage roadway

The bottom drainage roadway serves mainly to drain the gas from the No. 3 coal seam. To improve the effectiveness of gas drainage, it is necessary to determine the initial sealing depth of the borehole (the distance between capsular bag 1 and the collar in Figure 12). Generally, to ensure that there is no air leakage during gas drainage, the position of capsular bag 1 should be beyond the edge of the roadway's plastic zone (Figure 12). Therefore, determining the plastic zone range of the roadway is crucial for ensuring the sealing effect of the borehole.

Analysis of drilling chips data is a common method to determine the plastic zone range of roadways. The number and size of drill chips are indicative of the *in-situ* stress – a smaller number of larger chips indicates less ground stress in the area. During drilling, cuttings can be collected every 1 m, and the depth of the roadway's plastic zone can be determined by examining the changes in the size of the drilled chips at different positions.

A 42 mm rotary drilling rod was used to obtain the drilling cuttings by drilling crosscutting boreholes perpendicular to the No. 3 coal seam from the bottom drainage roadway of the 1301 workface. The results (average mass of drill cuttings) are shown in Figure 13. When the drilling operations reached 7 m from the roadway's edge, the mass of drill cuttings increased, indicating that stress concentration occurs around the roadway at this position. At a depth of 8 m, the mass of drill cuttings peaked (indicating maximum fracturing), showing that the stress concentration had also peaked at this position. At a depth of 9 m, the mass of drill chips decreased significantly, indicating that the rock surrounding the roadway at that position was gradually returning to the original stress state. This shows that the plastic zone of the bottom drainage roadway of the 1301 workface extends to 8 m. In the process of gas drainage, to avoid air leakage from the borehole, the initial sealing depth of each borehole should be greater than 8 m.

Technical advantages of underground gas drainage methods

Surface wells can also be used for gas drainage. However, for coal and gas outburst-prone coal seams, mines in China mainly adopt underground gas drainage methods. The main reasons are as follows:

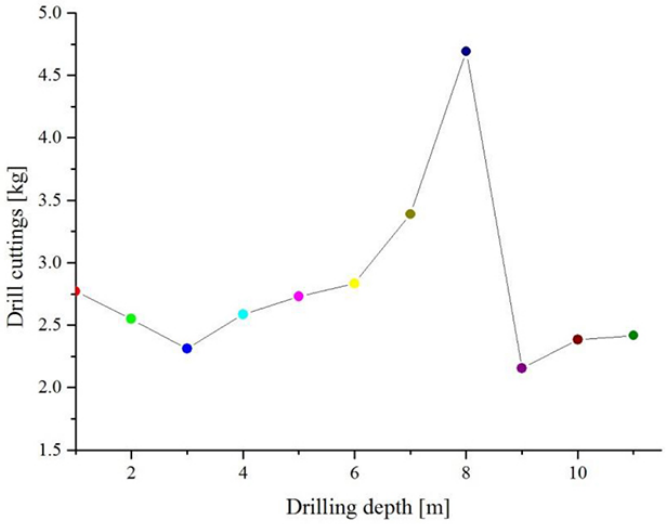

Figure 13—Drill cuttings masses at different positions around the bottom drainage roadway

- Owing to the influence of topography, the surface wells are unevenly arranged, unlike underground boreholes drainage.
- The area close to the surface well has a good drainage effect. Conversely, the area far from the surface well has poor drainage effect. When the drainage time is short, the gas drainage balance is poor and the reliability is low.
- All measures are implemented on the ground. The State not only does not have test standards for surface well pre-drainage, but it is also difficult to test.
- The cost of surface well drainage is also higher than that for underground borehole drainage.

Conclusions

The optimum location of the bottom drainage roadway for gas drainage was determined by using a combination of geological surveys and numerical simulations.

1. Geological exploration drilling around the mining workface showed that the vertical distance between the bottom drainage roadway and the mining workface was 14 m. A marker bed exists at this position, and the roadway can be easily maintained. The coal seam would not be accidentally exposed during the excavation of the bottom drainage roadway.
2. According to the statistical data on outburst-prone mines in China, combined with the numerical simulation, the bottom drainage roadway should be located 20 m outside the mining workface 'footprint' on the horizontal projection. At this position, the bottom drainage roadway will be away from the stress concentration area while the workface is being mined, facilitating roadway maintenance. Also, the length of the crosscutting boreholes is relatively short, which reduces the amount and costs of drilling.
3. In the process of gas drainage, to avoid air leakage from the boreholes, the initial sealing depth of the borehole should be greater than 8 m.

Acknowledgments

This work was supported by the National Natural Science Foundation of China (51804102), the Henan Key Laboratory of Coal Green Conversion (CGCF201809), the State Key Laboratory Cultivation Base for Gas Geology and Gas Control of Henan Province (WS2019B12), the Program for Innovative Research Team of Henan Polytechnic University (T2019-4), and the Fundamental Research Funds for the Universities of Henan Province (NSFRF170901).

Author contributions

Haidong Chen and Fenghua An wrote the main manuscript; Haidong Chen carried out the study and prepared all the figures; Zhaofeng Wang and Xiangjun Chen supervised the study. All authors reviewed the manuscript.

References

Bai, Q.S., Tu, S.H., Zhang, C., and Zhu, D.F. 2016. Discrete element modeling of progressive failure in a wide coal roadway from water-rich roofs. *International Journal of Coal Geology*, vol. 167. pp. 215-229.

Chen, H.D., Chen, X.J., Wang, Z.F., Li, Z.Q., and An, F.H. 2020. Plastic zone range of a roadway considering the creep effect. *Scientific Reports*, vol. 10. pp. 20341.

Chen, H.D., Cheng, Y.P., Ren, T., Zhou, H.X., and Liu, Q.Q. 2014. Permeability distribution characteristics of protected coal seams during unloading of the coal body. *International Journal of Rock Mechanics and Mining Sciences*, vol. 71. pp. 105-116.

Chen, H.D., Wang, Z.F., Chen, X., Chen, X.J., and Wang, L.G. 2017. Increasing permeability of coal seams using the phase energy of liquid carbon dioxide. *Journal of CO_2 Utilization*, vol. 19. pp. 112-119.

Chen, Y.X., Xu, J., Peng, S.J., Yan, F.Z., and Fan, C.J. 2018. A gas–solid–liquid coupling model of coal seams and the optimization of gas drainage boreholes. *Energies*, vol. 11. pp. 560.

Cheng, Y.P. 2010. Theory and Engineering Application of Coal Mine Gas Prevention and Control. China University of Mining and Technology Press, Xuzhou, China.

Cheng, Y.P., Wang, L., and Zhang, X. 2011. Environmental impact of coal mine methane emissions and responding strategies in China. *International Journal of Greenhouse Gas Control* , vol. 5. pp. 157-166.

China State Administration of Work Safety. 2019. Detailed Rules for Prevention and Control of Coal and Gas Outburst. China Coal Industry Press, Beijing, China.

Coggan, J., Gao, F.Q., Stead, D., and Elmo, D. 2012. Numerical modelling of the effects of weak immediate roof lithology on coal mine roadway stability. *International Journal of Coal Geology*, vol. 90-91. pp. 100-109.

Dejean, M.J.P. 1976. Deformation analysis in underground roadways. *International Journal of Rock Mechanics and Mining Sciences & Geomechanics Abstracts*, vol. 13. pp. 25-30.

Guo, H., Yuan, L., Shen, B., Qu, Q., and Xue, J. 2012. Mining-induced strata stress changes, fractures and gas flow dynamics in multi-seam longwall mining. *International Journal of Rock Mechanics and Mining Sciences* , vol. 54. pp. 129-139.

Hu, S. and Liu, H. 2016. Leakage mechanism of coal seam gas drainage borehole and its application research progress. *Safety in Coal Mines*, vol. 47. pp. 170-173 [in Chinese].

Islam, M.R. and Shinjo, R. 2009. Numerical simulation of stress distributions and displacements around an entry oadway with igneous intrusion and potential sources of seam gas emission of the Barapukuria coal mine, NW Bangladesh. *International Journal of Coal Geology*, vol. 78. pp. 249-262.

Itasca Consulting Group. 2005. FLAC3D User's Guide. Minneapolis, MN.

Jiang, L.J., Mitri, H.S., Ma, N.J., and Zhao, X.D. 2016. Effect of foundation rigidity on stratified roadway roof stability in underground coal mines. *Arabian Journal of Geoscience*, vol. 9. pp. 32-44.

Jiang, J.Y., Yang, W.H., Cheng, Y.P., Liu, Z.D., Zhang, Q., and Zhao K. 2019. Molecular structure characterization of middle-high rank coal via XRD, Raman and FTIR spectroscopy: Implications for coalification. *Fuel*, vol. 239. pp. 559-572.

Kong, S.L., Cheng, Y.P., and Liu, H. 2014. A sequential approach to control gas for the extraction of multi-gassy coal seams from traditional gas well drainage to mining-induced stress relief. *Applied Energy*, vol. 131. pp. 67-78.

Li, H., Feng, Z.C., Zhao, D., and Duan, D. 2017. Simulation experiment and acoustic emission study on coal and gas outburst. *Rock Mechanics and Rock Engineering*, vol. 50. pp. 2193-2205.

Li, Y. and Li, H. 2015. Measurement and analysis of roadway deformation of floor roadway. *Coal Mine Modernization*, vol. 2. pp. 26-28 [in Chinese].

Liu, X.J., Li, X.M., and Pan, W.D. 2016. Analysis on the floor stress distribution and roadway position in the close distance coal seams. *Arabian Journal of Geoscience*, vol. 9. pp. 83-95.

Liu, Z., and Zhang, S. 2018. Study on rational layout of floor gas drainage gateway in high gassy outburst seam. *Coal Science and Technology*, vol. 46. pp. 155-160 [in Chinese].

Lu, S., Li, L., Cheng, Y., Sa, Z., Zhang, Y., and Yang, N. 2017. Mechanical failure mechanisms and forms of normal and deformed coal combination containing gas: Model development and analysis. *Engineering Failure Analysis*, vol. 80. pp. 241-252.

Lu, S., Zhang, Y., Sa, Z., and Si, S. 2019. Evaluation of the effect of adsorbed gas and free gas on mechanical properties of coal. *Environmental Earth. Sciences*, vol. 78. pp. 218.

Nan, H., Li, M., and Guan, X. 2015. Optimization research on floor drainage lane position in outburst coal seam. Environ. *Environmental Journal of Henan Polytechnic University*, vol. 34. pp. 463-467 [in Chinese].

Pan, R., Ma, Z., Yu, M., and Wu, S. 2019. Research on the deformation characteristics and support technology of a bottom gas extraction roadway under repeated interference. *Advances in Civil Engineering*, vol. 2019. pp. 1413568.

Sun, Y., Lu, W., Yang, K., Zhou, C., and Huang, X. 2015. Study on disposal technology of air leakage around borehole by three-pouch closure device. *Journal of Safety Science and Technology*, vol. 11. pp. 67–72 [in Chinese].

Wang, H.F., Cheng, Y.P., Wang, W., and Xu, R. 2014. Research on comprehensive CBM extraction technology and its applications in China's coal mines. *Journal of Natural Gas Science and Engineering*, vol. 20. pp. 200-207.

Wang, H.W., Jiang, Y.D., Xue, S., Shen, B.T., Wang, C., Lv, J.G., and Yang, T. 2015. Assessment of excavation damaged zone around roadways under dynamic pressure induced by an active mining process. *International Journal of Rock Mechanics and Mining Sciences*, vol. 77. pp. 265-277.

Wang, L., Chen, X.J., Wang, Z., Xu, S., and Xu, Q. 2020. Extending the protection range in protective seam mining under the influence of gas drainage. *Journal of the Southern African Institute of Mining and Metallurgy*, vol. 120, no. 3. pp. 211-220.

Whittaker, B.N. and Singh, R.N. 1981. Stability of longwall mining gate roadways in relation to rib pillar size. *International Journal of Rock Mechanics and Mining Sciences & Geomechanics Abstracts*, vol. 18. pp. 331-334.

Xiao, T.Q., Wang, X.Y., and Zhang, Z.G. 2014. Stability control of surrounding rocks for a coal roadway in a deep tectonic region. *International Journal of Mining Science and Technology*, vol. 24. pp. 171-176.

Xie, J.L. and Xu, J.L. 2015. Ground penetrating radar-based experimental simulation and signal interpretation on roadway roof separation detection. *Arabian Journal of Geoscience*, vol. 8. pp. 1273-1280.

Xue, S., Yuan, L., Wang, Y., and Xie, J. 2014. Numerical analyses of the major parameters affecting the initiation of outbursts of coal and gas. *Rock Mechanics and Rock Engineering*, vol. 47. pp. 1505-1510.

Yang, D., Chen, Y., Tang, J., Li, X., Jiang, C., Wang, C., and Zhang C. 2018. Experimental research into the relationship between initial gas release and coal-gas outbursts. *Journal of Natural Gas Science and Engineering*, vol. 50. pp. 157-165.

Yang, S.Q., Chen, M., Jing, H.W., Chen, K.F., and Meng, B. 2017. A case study on large deformation failure mechanism of deep soft rock roadway in Xin'An coal mine, China. *Engineering Geology*, vol. 217. pp. 89-101.

Yang, X., Wen, G., Sun, H., Li, X., Lu, T., Dai, L., Cao, J., and Li, L. 2019. Environmentally friendly techniques for high gas content thick coal seam stimulation – multi-discharge CO_2 fracturing system. *Journal of Natural Gas Science and Engineering*, vol. 61. pp. 71-82.

Yu, B., Su, C., and Wang, D. 2015. Study of the features of outburst caused by rock cross-cut coal uncovering and the law of gas dilatation energy release. *International Journal of Mining Science and Technology*, vol. 25. pp. 453-458.

Zhang, H.L., Cao, J.J., and Tu, M. 2013. Floor stress evolution laws and its effect on stability of floor roadway. *International Journal of Mining Science and Technology*, vol. 23. pp. 631-636.

Zhang, K., Zhang, G.M., and Hou, R.B. 2015. Stress evolution in roadway rock bolts during mining in a fully mechanized longwall face, and an evaluation of rock bolt support design. *Rock Mechanics and Rock Engineering*, vol. 48. pp. 333-344.

Zhou, H.X., Yang, Q., Cheng, Y.P., Ge, C., and Chen, J. 2014. Methane drainage and utilization in coal mines with strong coal and gas outburst dangers: A case study in Luling mine, China. *Journal of Natural Gas Science and Engineering*, vol. 20. pp. 357-365. ◆